JOINT TRACKING GPS AND LEO SIGNALS WITH ADAPTIVE VECTOR TRACKING LOOP IN CHALLENGING ENVIRONMENTS

Guangrui Liu, Lei Wang

State Key Laboratory of Information Engineering in Surveying, Mapping and Remote Sensing, Wuhan University
Contacts: lei.wang@whu.edu.cn

Commission III, WG III/1

KEY WORDS: Signal Tracking, LEO, Navigation, Vector Tracking loop, Weak Signals.

ABSTRACT:

Navigation from LEO satellites own many merits and attracts increasing popularity recently. In addition to increasing the signal availability, the low signal strength loss and fast satellite geometry change from LEO satellite are particularly appealing in challenging environments. Recently, a few researchers attempt to navigate with non-cooperative signals from LEO satellites with pure phase lock loop (PLL) or frequency lock loop (FLL), while a more practical solution to utilizing LEO navigation is joint positioning with the existing GNSS signals which has not been seriously studied. In this study, we proposed a joint GPS and LEO navigation signal tracking strategy that employs a vector tracking loop (VTL) with fully considering the high dynamic characteristics of the LEO signals. In order to solve the high dynamics problem, the second-order deviation parameters were considered in the extended Kalman filter, which is more adaptive to the non-linear variation of the signal acceleration. In addition, a carrier-to-noise ratio (C/N0) based observation noise determination strategy is employed to adapt different observation conditions. The proposed method was verified with different simulation data and the results indicate the adaptive vector tracking loop is capable of tracking GPS and LEO signals simultaneously and robustly. The benefit is particularly in the weak signal scenarios. The experiment results also reveal that the joint vector tracking loop improves positioning accuracy in GNSS challenging environments.

1. INTRODUCTION

Global navigation satellite systems (GNSS) have been widely utilized to facilitate people's lives and increase productivity. However, GNSS cannot work well in many challenging environments, such as the obstructions from canopies and bridges, the multipath caused by buildings and urban canyons and so on. To solve these problems, some researchers proposed the low earth orbit satellites(LEO) navigation augmentation system and this system contains two preferable perspectives: stronger power for navigation and a large LEO constellation for navigation augmentation(Li, Xu, Guan, Gao, & Jiang, 2021).
In recent years, many corporations have launched their own LEO communication satellites constellations, such as Starlink, Iridium, OneWeb, etc. Those LEO communication satellites increased the numbers of satellites in low earth orbit and have advantages over making up visible satellite numbers in urban canyons. For the existing commercial communication LEO satellites, navigation information was not modulated in their signal structure so few researchers attempt to calculate the receiver's position with pure Doppler measurements. Orabi, Khalife, and Kassas (2021) and Kassas, Khalife, and Neinavaie (2021) have successfully demonstrated the possibility of positioning using the commercial communication LEO satellites to determine positions with Doppler measurements. Those researches reflected the possibility and superiority of communication LEO satellites, however, there is little research about the supremacy in the position of LEO satellites with navigation information signal structure under challenging environments. In 2018, Wuhan University (Wang et al., 2018) launched a scientific experimental satellite, called Loujia-1A satellite, and demonstrated that LEO satellites with navigation information have advantages in fast-changing geometry and low free space signal loss compared with current MEO/GEO based GNSS.

Compared to GNSS satellites, LEO satellites move fast, which potentially causes high dynamic problems in the line-of-sight(LOS) direction and signal tracking loop unstable. For a scalar tracking loop, the range of GNSS signal noise bandwidth is 5-20Hz ideally while the noise bandwidth of LEO signal is up to 80Hz, due to the LEO signal Doppler is ±40kHz. Therefore, it is easy to lose-of-lock and causes large observation noise in the tracking loop. And the noisy signal would affect the code phase accuracy and ephemeris decoding. For those reasons, the vector tracking loop (VTL) is the prior choice for the high dynamic signal problem. While the present model of vector loop builds up based on GNSS satellites and high-speed vehicles, those models could solve the high dynamic problem caused by vehicles not by LEO satellites(Lashley, Bevly, & Hung, 2009; Liu, Cui, Lu, & Feng, 2013; Won & Eissfeller, 2013). Hence, there is short of appropriate signal tracking method to solve the dynamic problem engendered by high-speed satellites.

From the above perspectives, this study will propose a novel dynamic model based on extended Kalman filter (EKF) to mitigate the high dynamic effect in LEO satellites signals. At the same time, considering the existing GNSS and actual application scenario, this study chooses to join tracking the LEO and GPS signal together to prove the strengths of LEO satellites in aiding GNSS signal tracking in challenging environments.

2. VECTOR TRACKING LOOP

LEO satellites signal power is stronger than MEO signal, and it could suffer less effect by obstructions. Its carrier-to-noise ratio

(C/N0) value could up to 55 dB-Hz. This advantage drives researcher to apply LEO signal in the challenging environments. However, the key problem of LEO signal is its high-dynamic feature which may destroy the stability of the tracking loop (Wang et al., 2019). Hence, the scalar tracking loop (STL) is not suitable for LEO signal tracking, and the vector tracking loop have more better robustness (Liu et al., 2013; Vila-Valls, Closas, Navarro, & Fernandez-Prades, 2017; Won & Eissfeller, 2013; Yan et al., 2014).

LEO signals containing navigation information have the following structure:

$$s_{IF,I}(n) = Ax(n)D(n)\cos(\varphi(n)) \quad (1)$$

$$s_{IF,Q}(n) = Ax(n)D(n)\sin(\varphi(n)) \quad (2)$$

where $S_{IF,I}(n), S_{IF,Q}(n)$ = the intermediate frequency (IF) of In-Phase/Quadrature (I/Q) signal structure.

When this signal arrived receiver, it contains both the IF signal and the Doppler information as follows:

$$f_R = f_{IF} + f_d \quad (3)$$

$$f_d = -\frac{(v^S - v_R)}{\lambda_L} * I \quad (4)$$

where f_R = the observed signal frequency

f_{IF} = the intermediate frequency

f_d = the Doppler frequency

v^S , v_R = the satellites velocity and receiver velocity

I = a unit vector in line-of-sight direction

λ_L = the wavelength

The tracking loop cares about geometry changes between satellites and receiver, which could be measured by the loop discriminators. The measurement error cloud be represented as:

$$\Delta X = \begin{bmatrix} \Delta\theta \\ \Delta f \end{bmatrix} * \lambda_L \quad (5)$$

where $\Delta\theta$ = the output of the phase discriminator

Δf = the output of the frequency discriminator

ΔX = the measurement value of pseudo-range difference and velocity differences.

In the vector tracking loop, these measurements (in Equation(5)) could be mapped to the position differences and the velocity differences, as shown in Equation(6):

$$\Delta X_{LOS} = \begin{bmatrix} p^S - p_R \\ v^S - v_R \end{bmatrix} * I \quad (6)$$

where p^S, p^R = the position of the satellite and the position of the receiver

v^S, v^R = the velocity of the satellite and the velocity of the receiver

ΔX_{LOS} = the position differences and the velocity differences between satellites and receiver mapped to the line-of-sight direction.

Equation(4), Equation(5) and Equation(6) indicate the relationship of loop measurement value and geometry change between satellites and receiver. This mapping relation could be accomplished in the vector tracking loop.

As shown in the Figure1, the vector tracking loop structure could directly estimate the receiver state according to the loop measurement. Firstly, ΔX_{LOS} gives the estimated value of the pseudo-rang and the estimated value of velocity in LOS direction and is mapped to local replication signal. After local replication signal mixing with the present IF signal, secondly, the discriminator measures difference and maps to pseudo-range difference and velocity difference as ΔX . Finally, the EKF uses ΔX as innovation information to time-update the receiver move state directly.

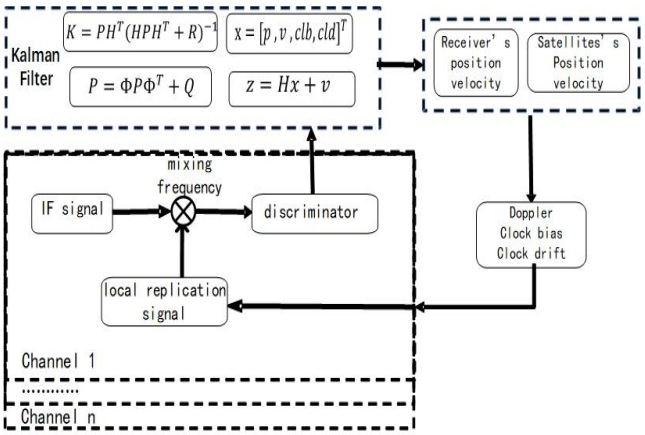

Figure 1. vector tracking loop structure

Expertly, multichannel vector tracking loop also could eliminate the receiver clock error and compensate the difference of geometry changes between the MEO satellites and the LEO satellites. Hence, these advantages contribute to the joint tracking GPS and LEO signals.

3. AN ADAPTIVE EKF CARRIER TRACKING LOOP

An optimal filter should be able to eliminate the signal noise and estimate the receiver's state vector $X_R = [p_R, v_R, t_R]^T$ by using the code phase and carrier frequency measurements obtained from the loop discriminator (in Equation(5)). In much research, the EKF model has nice performance in tracking high-dynamic signals. However, these EFK models care about the high-dynamic problems caused by high-speed receiver not by the LEO satellites. These present EKF models' measurement matrix (H matrix) could not reflect dramatic geometry changes between the LEO satellites and the receiver.

In this section, we proposed a novel EKF-based framework to solve the high dynamic problem in LEO satellite signal tracking and a stochastic model optimization to adaptively adjust noise matrix to adapt the challenging environment.

3.1 The Adaptive EKF MODEL for LEO Signal Tracking

In an EKF model, the estimation error is represented as:

$$\tilde{x}(k|k-1) = x(k) - \hat{x}(k|k-1) \tag{7}$$

where $x(k|k-1)$ = the estimation states value derived from $x(k-1)$ which respects the states of the receiver in $k-1$ epoch. The prior receiver state vector is given as $x(0|0) = [p_0, v_0, t_0]^T$ and the time-update procedure can be expressed as:

$$\hat{x}(k|k-1) = A\hat{x}(k-1|k-1) \tag{8}$$

$$P(k|k-1) = AP(k-1|k-1)A^T + Q \tag{9}$$

where A = the state transformation matrix (STM)
$P(k-1|k-1)$ = the variance-covariance matrix of the state in k-1 epoch
Q = the process noise matrix.

The state matrix and the variance-covariance matrix updating equations are given as

$$\hat{x}(k|k) = \hat{x}(k|k-1) + K(k) * \nu(k) \tag{10}$$

$$P(k|k) = \left[I - K(k) * H(k)\right] * P(k-1) \tag{11}$$

where $\nu(k)$ is the innovation vector, which can be get from loop discriminator as $\triangle X$ in Equation(5), $K(k)$ is the Kalman gain matrix, and $H(k)$ is the measurement matrix.

In standard EKF, the measurement matrix parameters are first-order Taylor expansion coefficient which could only reflect the high-speed changes caused by receivers not by satellites. In an EKF model for LEO signal tracking, the measurement matrix parameters should reflect the dramatic geometry changes in the LOS direction. In our novel EKF model, the $H(k)$ matrix was extended to second-order deviation so that it could deal with the speed variation of the LEO satellites, and it is expressed as:

$$H(i,k) = \begin{bmatrix} h_{p,x}, & h_{p,y}, & h_{p,z}, & 0, & 0, & 0, \\ \dot{h}_x, & \dot{h}_y, & \dot{h}_z, & h_{v,x}, & h_{v,y}, & h_{v,z}, \end{bmatrix} \tag{12}$$

where $\left[h_{p,x}, h_{p,y}, h_{p,z}\right]$ = the first-order Taylor expansion coefficient of the positions
$\left[h_{v,x}, h_{v,y}, h_{v,z}\right]$ = the first-order Taylor expansion coefficient of the velocities
$\left[\dot{h}_x, \dot{h}_y, \dot{h}_z\right]$ = the second-order Taylor expansion coefficient.

In order to incorporate the LEO high dynamic signal For LEO satellites signal, the second-order deviation parameters can be expressed as:

$$\begin{cases} \dot{h}_x = -\left(Vx_k^S - Vx_{(k|k-1)}^R\right) \times \dfrac{\left(Py_k^S - Py_{(k|k-1)}^R\right)^2 + \left(Pz_k^S - Pz_{(k|k-1)}^R\right)^2}{\|P_k^S - P_{(k|k-1)}^R\|^3} \\ \dot{h}_y = -\left(Vy_k^S - Vy_{(k|k-1)}^R\right) \times \dfrac{\left(Px_k^S - Px_{(k|k-1)}^R\right)^2 + \left(Pz_k^S - Pz_{(k|k-1)}^R\right)^2}{\|P_k^S - P_{(k|k-1)}^R\|^3} \\ \dot{h}_z = -\left(Vz_k^S - Vz_{(k|k-1)}^R\right) \times \dfrac{\left(Px_k^S - Px_{(k|k-1)}^R\right)^2 + \left(Py_k^S - Py_{(k|k-1)}^R\right)^2}{\|P_k^S - P_{(k|k-1)}^R\|^3} \end{cases} \tag{13}$$

where $[P_x, P_y, P_z], [V_x, V_y, V_z]$ = the position and velocity in the Earth-Centre-Earth-Fixed (ECEF) frame
$\| \|$ = the distance between satellite and receiver.

3.2 Stochastic Model Optimization

Though the above EKF model solve high-dynamic signal problem, the measurement noise still unavoidably exists in the vector tracking loop especially in harsh environment. This section will talk about a stochastic model optimization that could adaptively adjust noise covariance matrix to adapt the challenging environment.
In Equation(10) and Equation(11), $K(k)$ could affect the value of the state matrix and it contains the measurement noise so that it is expressed as:

$$K(k) = \frac{P(k-1) * H(k)^{'}}{\left(H(k) * P(k-1) * H(k)^{'} + R(k)\right)} \tag{14}$$

where $R(k)$ = the measurement noise covariance

The measurement noise covariance involves code phase and carrier phase error noise. If there is no relationship between the code phase error and carrier frequency error, the matrix $R(k)$ would be a diagonal matrix and the element in the diagonal line depends on the present signal carrier-to-noise ratio (C/N0). In a challenging environment, measurement noise would change greatly for the signal sheltered or interfered. Hence, it is essential to design a dynamic matrix $R(k)$ that could automatically adapt Kalman Filter's gain to environmental change.

$$R(k) = \begin{bmatrix} \mathrm{var}_1 & & & \\ & \mathrm{var}_2 & & \\ & & \ddots & \\ & & & \mathrm{var}_n \end{bmatrix} \tag{15}$$

where $\mathrm{var}_i, i = 1...n$ = the measurement noise covariance
n = the number of signal channels.

The var_i can be expressed as following equations:

$$\begin{cases} \alpha_E = CN0 * \tau * code^2{}_E \\ \alpha_L = CN0 * \tau * code^2{}_L \end{cases} \tag{16}$$

$$var = \frac{(\alpha_E + \alpha_L) * (\alpha_E - \alpha_L)^2 + (\alpha_E - \alpha_L) * (\alpha_E + \alpha_L)^2}{(\alpha_E + \alpha_L)^4} \tag{17}$$

where $CN0$ = the carrier-to-noise ratio from real signal

τ = coherent integral time

$code_E$, $code_L$ are the feature parameters about the difference of code phase error and correlator spacing.

4. EXPERIMENTAL RESULTS

In order to verify the performance of the proposed filter, we carried out a simulation study and the results are discussed in this section.

4.1 Experiment Setup

In this study, we used software to simulate the joint LEO and GPS signal after the pattern of challenging environments. This simulation dataset endured 80 seconds and the parameters of simulation is in the Table 1.

Parameter	Value
Carrier Frequency	1575.42 MHz
Code Frequency	1.023 MHz
Modulation	BPSK
Simple Frequency	2.6 MHz

Table 1. the parameters of Signal Simulator

We set the signal simulator's parameters after the pattern of the harsh environment. Like in Figure 2, the GPS signal decreased 5dB every 15 seconds. Figure 3 shows the acquired satellites, where G1 to G9 were simulated GPS satellites and L1 to L3 were LEO satellites.

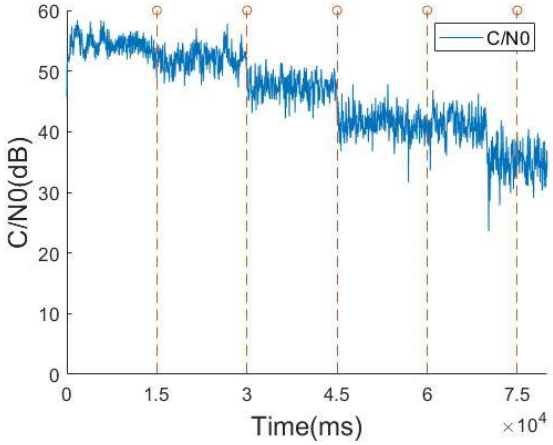

Figure 2. GPS signal C/N0

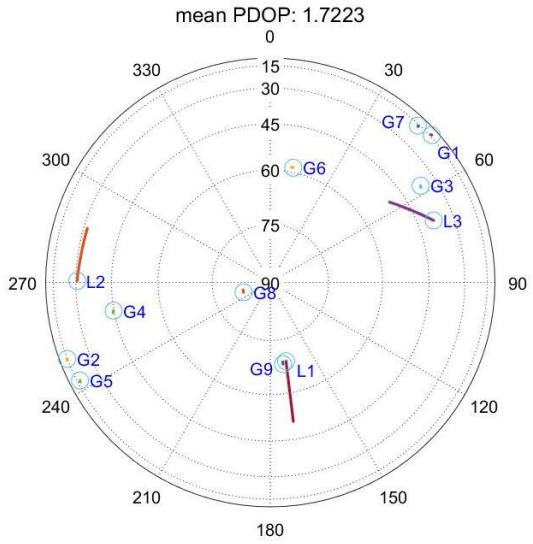

Figure 3. Sky-plot of the Simulated GPS/LEO satellites

4.2 Frequency Error Analysis

Figure 4 shows the carrier frequency of a GPS satellite, which had greatly changed in a challenging environment. The blue line means the tracking result from the scalar loop and the red line is on behalf of carrier frequency from the vector loop. This shows that the vector loop could smooth and revert frequency superiorly and reduce environmental noise. Reducing the noise in the tracking loop contributed to keeping a steady state of the loop and finding the frame header accurately.

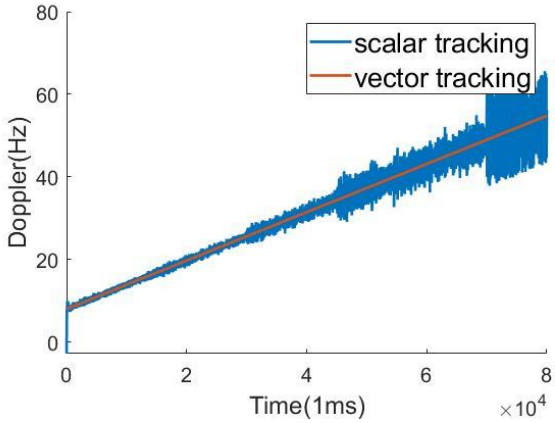

Figure 4. Carrier Frequency of a GPS satellite

The frequency stability is an important index to evaluate the loop performance. For a N-order frequency-locked loop, the theoretical frequency tracking error bound could be expressed as the follows:

$$f_e = \frac{d}{dt} * \left(\frac{1}{\omega_n^N} * \frac{d^N R}{dt^N}\right) = \frac{1}{\omega_n^N} * \frac{d^{N+1} R}{dt^{N+1}} \tag{18}$$

where f_e = the theoretical tracking error bound

R = the distance between satellites and receiver,

ω_n = the loop parameter set as 0.53 according to common parameters.

In 2nd -order frequency-locked loop, $\frac{d^3R}{dt^3}$ is the derivative of acceleration in line of sight, which changed with satellites' position and velocity.

As shown in Figure 5, the theoretical tracking error bound were 0.159 Hz, 0.183 Hz and 0.180 Hz, and the frequency error in the vector tracking loop was all in range of stable tracking error, while the scalar tracking loop frequency error was more than 50 percent of stable tracking error (in Figure 6).

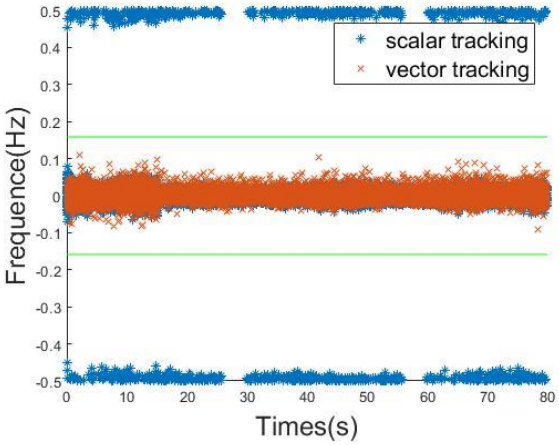

Figure 5. Comparison of VTL and STL frequency tracking error for L1 satellite

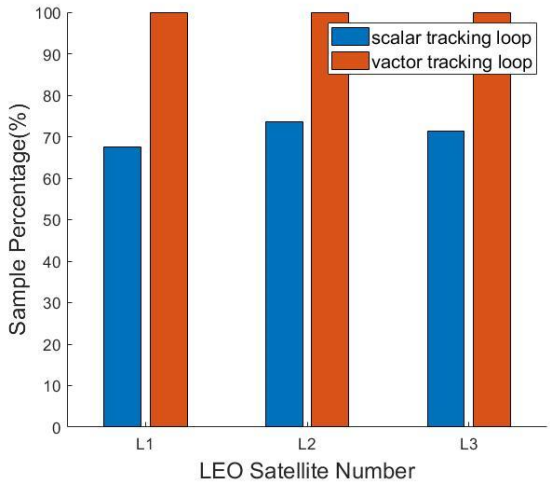

Figure 6. Comparison of the sample percentage within the frequency error bounds between VTL and STL

In Table 2, the standard deviation value (STD) of the vector tracking loop had an advantage over the value of the scalar tracking loop. When signal in high dynamic, this novel EKF vector tracking loop could offset and cover the loss of signal frequency and maintain loop steady state.

Satellites PRN	Vector tracking Std	Scalar Tracking Std
L01	0.0094	0.0608
L02	0.0180	0.0617
L03	0.0110	0.0623
G1	0.0807	0.0789
G2	0.0796	0.0773
G3	0.0824	0.0839
G4	0.1080	0.0961
G5	0.1161	0.1019
G6	0.1302	0.1297
G7	0.1360	0.1315
G8	0.1339	0.1287
G9	0.1378	0.1309

Table 2. Comparison of the standard deviation of the frequency error between VTL and STL

In Figure 7 and Table 3 show the standard deviation value of the code phase error, there was clear superiority in the vector tracking loop in the GPS satellites. It indicates that this AEKF vector tracking perform more well in the weak signal environment.

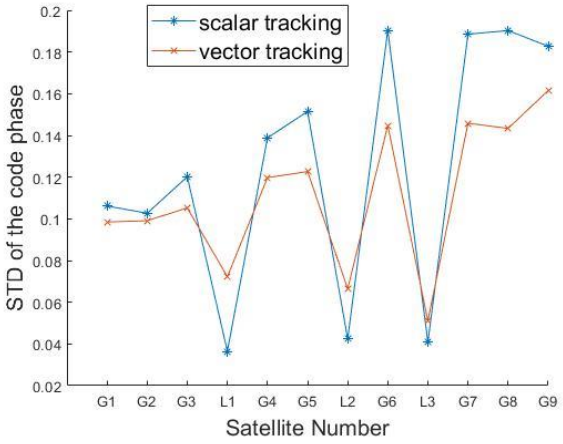

Figure 7. Comparison of the standard deviation of the code phase error between VTL and STL

Satellites PRN	Vector tracking Std	Scalar Tracking Std
G1	0.0985	0.1061
G2	0.0991	0.1027
G3	0.1052	0.1202
G4	0.1198	0.1388
G5	0.1227	0.1515
G6	0.1447	0.1904
G7	0.1458	0.1886
G8	0.1434	0.1903
G9	0.1615	0.1827
L1	0.0722	0.0365
L2	0.0664	0.0423
L3	0.0510	0.0408

Table 3. Comparison of the standard deviation of the code phase error between VTL and STL

5. CONCLUSION

Through the above sections, the results of experiments proved that this novel AEKF model has advantages in solving the problems of tracking dynamic signal and weak signals. Firstly, this filter could reduce the frequency error effectively, especially for the high-dynamic LEO signal. Secondly, for the weak GPS signal, this filter could reduce the code phase error and maintain loop stability and robustness even in the challenging environment.

In future works, we will focus on the phase analysis in EKF model vector tracking loop. Improving the accuracy of carrier phase measurements could enhance positioning accuracy.

Meanwhile, we will add more complex and challenging experimental scenarios to test this novel vector tracking loop's performance.

ACKNOWLEDGEMENTS

This work was sponsored by the National Natural Science Foundation of China (NSFC 42074036) and the Fundamental Research Funds for the Central Universities.

REFERENCES

Kassas, Z. Z., Khalife, J., & Neinavaie, M. (2021). The First Carrier Phase Tracking and Positioning Results with Starlink LEO Satellite Signals. *IEEE Transactions on Aerospace and Electronic Systems*, 1-1. doi:10.1109/taes.2021.3113880

Lashley, M., Bevly, D. M., & Hung, J. Y. (2009). Performance Analysis of Vector Tracking Algorithms for Weak GPS Signals in High Dynamics. *IEEE Journal of Selected Topics in Signal Processing, 3*(4), 661-673. doi:10.1109/jstsp.2009.2023341

Li, M., Xu, T., Guan, M., Gao, F., & Jiang, N. (2021). LEO-constellation-augmented multi-GNSS real-time PPP for rapid re-convergence in harsh environments. *GPS Solutions, 26*(1). doi:10.1007/s10291-021-01217-9

Liu, J., Cui, X., Lu, M., & Feng, Z. (2013). Vector tracking loops in GNSS receivers for dynamic weak signals. *Journal of Systems Engineering and Electronics, 24*(3), 349-364. doi:10.1109/jsee.2013.00044

Orabi, M., Khalife, J., & Kassas, Z. M. (2021). *Opportunistic Navigation with Doppler Measurements from Iridium Next and Orbcomm LEO Satellites*. Paper presented at the 2021 IEEE Aerospace Conference (50100).

Vila-Valls, J., Closas, P., Navarro, M., & Fernandez-Prades, C. (2017). Are PLLs dead? A tutorial on kalman filter-based techniques for digital carrier synchronization. *IEEE Aerospace and Electronic Systems Magazine, 32*(7), 28-45. doi:10.1109/maes.2017.150260

Wang, L., Chen, R., Li, D., Zhang, G., Shen, X., Yu, B., . . . Pan, Y. (2018). Initial Assessment of the LEO Based Navigation Signal Augmentation System from Luojia-1A Satellite. *Sensors, 18*(11). doi:10.3390/s18113919

Wang, L., Chen, R., Xu, B., Zhang, X., Li, T., & Wu, C. (2019). The Challenges of LEO Based Navigation Augmentation System – Lessons Learned from Luojia-1A Satellite. In *China Satellite Navigation Conference (CSNC) 2019 Proceedings* (pp. 298-310).

Won, J.-H., & Eissfeller, B. (2013). A Tuning Method Based on Signal-to-Noise Power Ratio for Adaptive PLL and its Relationship with Equivalent Noise Bandwidth. *IEEE Communications Letters, 17*(2), 393-396. doi:10.1109/lcomm.2013.01113.122503

Yan, K., Ziedan, N. I., Zhang, H., Guo, W., Niu, X., & Liu, J. (2014). Weak GPS signal tracking using FFT discriminator in open loop receiver. *GPS Solutions, 20*(2), 225-237. doi:10.1007/s10291-014-0431-3